




# Effect of fiber properties and dispersion management on distortions associated with two subcarriers modulation of laser diode in radio over fiber systems

Alaa Mahmoud<sup>1,a</sup> , Yasmin Abd El-Salam<sup>1</sup>, Moustafa Ahmed<sup>2,3</sup>, and Tarek Mohamed<sup>1</sup>

<sup>1</sup> Laser Institute for Research and Applications LIRA, Beni-Suef University, Beni Suef 62511, Egypt

<sup>2</sup> Department of Physics, Faculty of Science, Minia University, El-Minia 61519, Egypt

<sup>3</sup> Department of Physics, Faculty of Science, King Abdulaziz University, 80203, Jeddah 21589, Saudi Arabia

Received 27 July 2022 / Accepted 1 November 2022 / Published online 29 November 2022  
© The Author(s) 2022

**Abstract.** We present numerical modeling and simulation on the effects of standard single-mode fiber (SSMF) properties and different dispersion management approaches on the distortions of laser diode. These distortions are associated with the two-tone modulation of laser diode for use in radio over fiber systems. The fiber properties include attenuation and dispersion. The dispersion management approaches include the use of nonzero dispersion-shifted fiber (NZ-DSF), fiber Brag grating (FBG), and dispersion-compensating fiber (DCF). The laser is directly modulated with two analog frequencies of 25 and 25.1 GHz at different modulation depths ( $m$ ). The modulated laser signals are then propagated through SSMF at different lengths ( $L$ ). The investigated laser signal distortions include the 2nd harmonic distortion (HD2), and the 2nd and 3rd intermodulation distortions (IMD2 and IMD3, respectively). The results reveal that all laser distortions are exacerbated as the fiber length increases, which is mainly due to the chromatic dispersion, while fiber attenuation has no effect. The use of dispersion management approaches gives almost similar effects on the reduction of IMD3 when  $L = 1$  km, regardless of the value of  $m$ . Up to  $m = 0.3$ , DCF is the most effective approach for reducing all distortions over the entire fiber length range, while NZ-DSF is the least. When  $L = 2$  km, FBG is the most effective approach for reducing both IMD2 and HD2 when  $m \geq 0.4$ , whereas when  $L$  is increased to 6 km, DCF is the most effective approach up to  $m = 0.5$ .

## 1 Introduction

Radio over fiber (RoF) transmission systems are an appropriate technology for integrating optical and wireless systems. Also, they provide a wide coverage area without increasing the system complexity or cost [1]. Laser diodes (LDs) play an important role in the development of RoF systems due to their advantage of high bandwidth. Traditional LDs have a bandwidth of several GHz [2], which recently has been enhanced to > 20 GHz with the innovation of multiple quantum well lasers [3]. This development helps to transmit and distribute microwave or millimeter-wave signals over optical fibers. This, in turn, meets the rapid evolution of wireless technology to integrate frequency bands higher than those currently used. This great advantage motivates the use of fifth-generation mobile networks [4].

Direct modulation of LDs in the GHz range with two subcarriers (two tones) has recently attracted a lot of attention for increasing the information capacity and transmission speed in analog RoF systems [5–7]. This

is because direct modulation is a simpler, less expensive, and less power-consuming technique compared to external modulation [8–10]. However, directly modulated LDs introduce nonlinear dynamics associated with the laser resonance, such as gain suppression and hole burning. These dynamics strongly affect the light-current linearity of the laser due to the inhomogeneous pinning of the electron density in the laser cavity [11–13]. These nonlinear laser dynamics create undesired distortion products associated with the modulated laser signal, which degrades the transmission quality [14, 15]. Typically, the nonlinear distortions associated with analog two subcarriers modulation of LDs are harmonic distortions (HDs) and intermodulation distortions (IMDs) [16–19]. These distortions are exacerbated when the frequency of the fundamental signals approaches the relaxation frequency of the laser ( $f_{-r}$ ) [20–22]. In addition, SSMFs have the advantages of immunity to radio frequency interference and large bandwidth [23]. However, they have some issues, namely attenuation and chromatic dispersion that can affect the modulated laser signals by adding further degradations [24]. The dispersion-induced nonlinear distortions are one of the most significant dispersion penalties of the fiber. It

<sup>a</sup> e-mail: [alaa.abutaleb@lira.bsu.edu.eg](mailto:alaa.abutaleb@lira.bsu.edu.eg) (corresponding author)

affects the information capacity and transmission distance of the systems employing the direct modulation technique [15, 25–29]. The frequency chirping of directly modulated LDs interacts with chromatic dispersion of the SSMF causing distortions of the signal traveling over the fiber [29]. This depends on the subcarrier frequency and the modulation depth, as well as the fiber length [26].

However, the estimation and prediction of nonlinear distortions generated by the directly modulated LD are important issues and have been intensively researched [14–19]. It is necessary to minimize the dispersion effects of SSMF to reduce such distortions in order to increase the BL-product of the fiber link. Different approaches have been proposed in order to minimize the dispersion effects of SSMF in analog fiber transmission systems and hence improve the fiber link performance [30–36]. One approach is to replace the SSMF with NZ-DSF, which is designed to reduce the chromatic dispersion effects [30, 31]. Another approach that almost cancels SSMF dispersion is the use of DCFs. DCF is a compensating device with a negative dispersion value that is used with the SSMF to compensate for its positive dispersion value [32–34]. FBG has been recently developed as an approach that acts as an effective filter for selecting desired wavelengths and hence reduces the dispersion effects of SSMFs [35–37]. Although these approaches are effective and important for improving system performance, their application to control fiber dispersion was limited to the low-frequency analog RoF systems (MHz range). Moreover, to the best of the authors' knowledge, there is little research comparing all of these dispersion management approaches for microwave or millimeter-wave analog RoF systems. However, there are various studies comparing the use of DCF and FBG in order to identify the optimum approach that improve the performance of optical fiber system [38, 39]. In ref. [38], the authors confirmed that the use of DCF, although being more costly to implement than FBG, is a promising approach for improving system performance. The authors in [39] made a comparison between the use of DCF and FBG for three different types of optical modulation in a particular optical system. They found that the use of DCF overcomes FBG for all three types. Recently, other studies proposed a combined technique employing DCF with FBG for increasing compensation efficiency [40, 41]. A hybrid combination of DCF and FBG has been used in [40] in order to mitigate the dispersion effect and other nonlinearities of fiber in RoF systems. In ref. [41], the authors compared different techniques to reduce the pulse width and found that using the combined technique of DCF with FBG is more efficient than using DCF or FBG alone. Additionally, they found that using DCF achieves high efficiency than FBG. Reference [42] presented a novel compensation technique of dispersion effect mitigation using a combination of multistage FBG and DCF design, which has been successfully used for data transmission over long distances.

In this paper, we present comprehensive investigations on the signal distortions of LDs radiating a

directly modulated fiber link with two analog subcarrier signals in the GHz range for use in analog RoF systems. The effects of SSMF properties (attenuation and dispersion) on the laser nonlinear distortions (HD2, IMD2, and IMD3) are explored. In addition, a comparison of the effect of the different dispersion management approaches on the modulated laser signal distortion types is presented. The dispersion management approaches include negative or positive NZ-DSF, FBG, and DCF. The main aim of the paper is to explore the optimum dispersion management approach that minimizes the distortions in order to enhance the transmission performance of high-frequency analog fiber links. The study is based on numerical integration of the rate equation model of LDs excited by bias current in conjunction with two sinusoidal electrical RF signals at 25 and 25.1 GHz. The frequency spectra of the modulated laser signals are investigated in the free-running case, under the effects of fiber attenuation and dispersion, and under the effects of the different management approaches. The analysis is performed at different ranges of laser modulation depth and fiber length.

The paper is organized as follows: In Sect. 2, we present the theoretical model and the simulation methodology. In Sect. 3, the results and discussion are presented, and the conclusions are given in Sect. 4.

## 2 Theoretical model and methodology

### 2.1 Dynamic behaviors of LDs

The dynamic behavior of LDs under amplitude modulation is typically modeled through numerical integration of the following coupled rate equations that describe the time evolution of the injected carrier density  $N(t)$  and emitted photon density  $S(t)$  in the active region [43]:

$$\begin{aligned} \frac{dN(t)}{dt} &= \frac{I(t)}{eV} - \frac{N(t)}{\tau_c} - \frac{g_o(N(t) - N_o)}{1 + \varepsilon S(t)} S(t) \quad (1) \\ \frac{dS(t)}{dt} &= \frac{\Gamma g_o(N(t) - N_o)}{1 + \varepsilon S(t)} S(t) - \frac{S(t)}{\tau_p} + \frac{\Gamma \beta_{sp} N(t)}{\tau_c} \quad (2) \end{aligned}$$

where  $e$  is the electron charge,  $V$  is the volume of the active region,  $\tau_{-c}$  is the electron lifetime,  $g_{-o}$  is the gain slop constant,  $N_{-o}$  is the carrier density at transparency,  $\varepsilon$  is the gain suppression factor,  $\tau_{-p}$  is the photon lifetime,  $\Gamma$  is the optical confinement factor, and  $\beta_{-sp}$  is the fraction of spontaneous emission noise coupled into the lasing mode.

In the case of two-tone modulation, the injection current  $I(t)$  in Eq. (1) is given by the following form:

$$I(t) = I_b \{1 + m[\sin(2\pi f_{m1}t) + \sin(2\pi f_{m2}t)]\} \quad (3)$$

where  $I_{-b}$  is the bias current,  $m = I_{-m}/I_{-b}$  is the modulation depth,  $I_{-m}$  is the modulation current, and  $f_{-m1}$  and  $f_{-m2}$  are the modulation frequencies of the first and

second tone, respectively, with a frequency spacing  $\Delta f$ . The time variation of the laser output power  $P(t)$  is estimated from the emitted photon density  $S(t)$  using the relationship [43]:

$$P(t) = \frac{V\eta h\nu}{2\Gamma\tau_p} S(t) \tag{4}$$

where  $\eta$  is the differential quantum efficiency,  $\nu$  is the optical frequency, and  $h$  is the Planck's constant. The power spectrum  $P(f)$  of the modulated laser signal is calculated by the fast Fourier transformation (FFT) of  $P(t)$  over a finite time period  $T$  as [44]

$$P(f) = \frac{1}{T} \left| \int_0^T P(\tau) e^{-j\omega\tau} d\tau \right|^2 = \frac{\Delta t^2}{T} |\text{FFT}[P(t)]|^2 \tag{5}$$

where  $\Delta t$  is the time integration step. The nonlinear distortions of the modulated laser signals are calculated as follows. The power spectrum  $P(f)$  displays the powers of the fundamental frequencies ( $f_{-m1}$  and  $f_{-m2}$ ) as well as the generated distortion products, namely second harmonic frequencies ( $2f_{-m1}$ ,  $2f_{-m2}$ ,  $3f_{-m1}$ ,  $3f_{-m2}$ , etc.), and second and third intermodulation frequencies ( $f_{-m1} \pm f_{-m2}$ ,  $2f_{-m1} \pm f_{-m2}$ ,  $2f_{-m2} \pm f_{-m1}$ , etc.). The power ratio (in dBc) of the second harmonic to the fundamental modulation frequency quantifies the second harmonic distortions HD2 as [22]:

$$\text{HD2} = 10 \log_{10} \frac{P_{2f_{-m1}}}{P_{f_{-m1}}} \tag{6}$$

where  $P_{2f_{-m1}}$  and  $P_{f_{-m1}}$  are the peak powers at  $2f_{-m1}$  and  $f_{-m1}$ , respectively, whereas the intermodulation distortions, IMD2 and IMD3, are described as the power ratios (in dBc) of the intermodulation products  $f_{-m1} \pm f_{-m2}$  and  $f_{-m1} \pm \Delta f$ , respectively, to  $P_{f_{-m1}}$  and are expressed as follows [6, 22]:

$$\text{IMD2} = 10 \log_{10} \frac{P_{f_{-m1} \pm f_{-m2}}}{P_{f_{-m1}}} \tag{7}$$

$$\text{IMD3} = 10 \log_{10} \frac{P_{f_{-m1} \pm \Delta f}}{P_{f_{-m1}}} \tag{8}$$

where  $P_{f_{-m1} \pm f_{-m2}}$  and  $P_{f_{-m1} \pm \Delta f}$  are the peak powers at second and third intermodulation products.

### 2.2 Signal propagation down the fiber

When the laser signal is transmitted over SSMF of length  $L$  and attenuation coefficient  $\alpha_f$ , the output optical power from the fiber  $P_{\text{out}}(L)$  is related to the power  $P_{\text{in}}(0)$  launched into the fiber by Beer's law as follows [2]:

$$P_{\text{out}}(L) = P_{\text{in}}(0) \exp(-\alpha_f L) \tag{9}$$

Assuming the optical field ( $E$ ) maintains its polarization along the fiber propagation length, the pulse-envelope amplitude of the electric field is considered to vary slowly and arrive at the output end of the fiber after a delay time of  $L/v_g$ , where  $v_g$  is the group velocity. This results in a reduced time  $\tau = t - L/v_g \equiv t - \beta_{-1} L$ , where  $\beta_{-1}$  is the group delay time needed for propagating the wave over distance  $L$  with velocity  $v_g$ , and thus  $E = E(L, \tau)$ . A single-mode nonlinear Schrödinger equation is then used to describe the evolution of  $E(L, \tau)$  along the fiber as follows [45, 46]:

$$\frac{\partial E(L, \tau)}{\partial L} + \alpha_f E(L, \tau) + i\beta_2(\omega_o) \frac{\partial^2 E(L, \tau)}{\partial \tau^2} = 0 \tag{10}$$

where  $\beta_{-2}$  is the group velocity dispersion (GVD), which is responsible for the pulse broadening inside the fiber, and  $\omega_o$  is the reference frequency of the signal. The third term represents the first-order GVD that determines how much optical pulse would broaden on propagation inside the fiber. Equation (10) is commonly calculated by the split-step FFT method [45–47]. It is customary in optical communication systems that the frequency spread ( $\Delta\omega$ ) induced by GVD is determined by the range of wavelengths ( $\Delta\lambda$ ) emitted by the optical source. By using  $\omega = 2\pi c/\lambda$ , where  $c$  is the speed of light in vacuum, the dispersion parameter ( $D$ ) in units of ps/km/nm is given as:

$$D = \frac{d\beta_1}{d\lambda} = \frac{d}{d\lambda} \left( \frac{1}{v_g} \right) = -\frac{2\pi c^2}{\lambda^2} \beta_2 \tag{11}$$

It is worth noting that the optical pulses still experience broadening even at  $D = 0$  (i.e., when  $\lambda$  is zero-dispersion wavelength  $\lambda_{\text{ZD}}$ ) as an impact of the higher-order dispersion effects governed by the so-called dispersion slope  $S = dD/d\lambda$  [2, 48].

### 2.3 Dispersion management approaches

The first approach for dispersion management used in this paper is the replacement of SSMF with nonzero dispersion-shifted fiber NZ-DSF (i.e.,  $\lambda_{\text{ZD}}$  is shifted into the vicinity of  $\lambda_o = 1.55 \mu\text{m}$ ). NZ-DSF, which is suitable for operation at  $1.55 \mu\text{m}$ , is designed so that the GVD parameter  $D$  of SSMF ( $\sim 16.75 \text{ ps/nm/km}$ ) is reduced to be  $D \approx 4.5 \text{ ps/nm/km}$  (which is + NZ-DSF) or  $\approx -7.5 \text{ ps/nm/km}$  (which is - NZ-DSF). These dispersion parameter values are chosen to avoid the four-wave mixing (FWM) effect [49–52].

The second approach used in this paper for compensating the positive dispersion accumulated along the length of the SSMF is the use of DCF with a high negative dispersion parameter value, which is typically placed after SSMF [53–55]. The physics behind this dispersion management approach is simply understood by supposing each optical pulse propagating through two segments of fiber. The first is the SSMF with length  $L_{\text{SMF}}$  and group velocity dispersion  $\beta_{2\text{SMF}}$ , and the

second is DCF with length  $L_{DCF}$  and group velocity dispersion  $\beta_{2DCF}$ . The condition for complete dispersion compensation is thus

$$\beta_{2SSMF}L_{SSMF} + \beta_{2DCF}L_{DCF} = 0, \text{ or} \quad (12)$$

$$D_{SSMF}L_{SSMF} = -D_{DCF}L_{DCF}$$

where  $D_{SSMF}$  and  $D_{DCF}$  are the dispersion parameters of SSMF and DCF, respectively.  $D_{DCF}$  must be  $< 0$  (i.e., DCFs must have normal GVD) because the  $D_{SSMF}$  is positive for the standard telecommunication fibers at  $1.55 \mu\text{m}$  (i.e., SSMFs with anomalous GVD) [2]. In addition,  $L_{DCF}$  should be chosen to satisfy the condition that

$$L_{DCF} = -\frac{D_{SSMF}}{D_{DCF}}L_{SSMF} \quad (13)$$

For practical reasons, DCFs are designed as short as possible with high negative value of  $D_{DCF}$  in order to minimize the cost [45]. In this paper,  $D_{DCF}$  is set as large as  $-82 \text{ ps/nm/km}$  with a small value of  $L_{DCF}$  satisfying the condition in Eq. (13) [2, 54–56].

FBG is the third approach used in this paper to manage the dispersion effect of SSMF. FBG is an optical reflection filter formed in a small segment of the fiber, which reflects a specific wavelength and transmits all others [2]. The propagated light in FBG is reflected by the grating according to the Bragg wavelength ( $\lambda_B$ ) [2].

$$\lambda_B = 2\tilde{n}\Lambda \quad (14)$$

where  $\tilde{n}$  is the average refractive index of the fiber core and  $\Lambda$  is the grating period. In the case of chirped gratings, the optical period  $\tilde{n}\Lambda$  varies over their length by varying either  $\tilde{n}$  or  $\Lambda$  [57]. As a result,  $\lambda_B$  varies along the grating, and thus, different wavelength components of an incident optical pulse are reflected at different points, which depend on the point where the Bragg condition is locally satisfied [2]. The physical concept underlying the use of FBG to compensate

for the dispersion effect of SSMF is explained as follows. The anomalous GVD of the SSMF at  $1.55 \mu\text{m}$  (where the shorter wavelength components travel faster than the longer ones) can be reduced by designing the FBG so that it provides normal GVD (where the shorter wavelength components reflected slower than the longer ones). In chirped FBG, the shorter wavelengths reflected from the shorter optical period  $\tilde{n}\Lambda$  (i.e., shorter  $\lambda_B$ ) take longer time, while the longer wavelengths reflected from the longer one (i.e., longer  $\lambda_B$ ) take shorter time. The round-trip time inside the grating, which represents the group-delay time inside FBG, is typically given by,

$$\tau_g = \frac{2\tilde{n}L_g}{c} \quad (15)$$

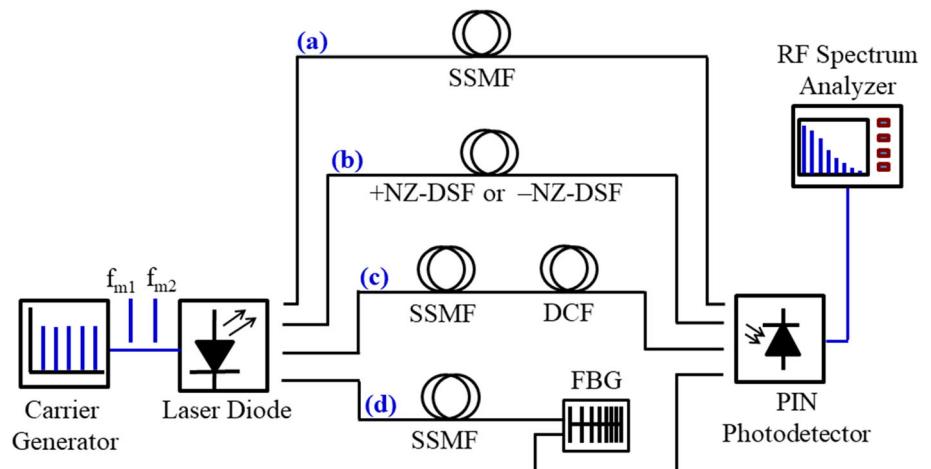
where  $L_g$  is the grating length. Assuming that the optical period varies linearly along its length, the dispersion parameter of the FBG ( $D_g$ ) can be determined as [2, 57]

$$D_g = \frac{\tau_g}{L_g\Delta\lambda_B} = \frac{2\tilde{n}}{c\Delta\lambda_B} \quad (16)$$

where  $\Delta\lambda_B$  ( $= \text{long } \lambda_B - \text{short } \lambda_B$ ; short  $\lambda_B \leq \lambda_o \leq \text{long } \lambda_B$ ,  $\lambda_o$  being the center wavelength) represents the difference in the  $\lambda_B$  at the two ends of the grating. FBG approach for dispersion compensation is accomplished in this paper by adjusting  $D_g$  to be  $< 0$  and equal the total dispersion of SSMF ( $\approx D_{SSMF}L_{SSMF}$ ).

The above theoretical model is simulated by using the Optisystem software. The proposed simulation setup of RoF transmission system is schematically illustrated in Fig. 1. The carrier generator is used to generate two sinusoidal electrical radio frequencies ( $f_{m1} = 25 \text{ GHz}$  and  $f_{m2} = 25.1 \text{ GHz}$ ). The laser diode is then directly modulated by injecting the current  $I(t)$  according to Eq. (3);  $I_b$  is injected directly in conjunction with  $I_m$ , which is formed with the sinusoidal signals generated by the carrier generator. The modulated laser signal is then transmitted through SSMF, which represents

**Fig. 1** The proposed simulation setup of RoF transmission system for two-tone direct modulation of laser diode when using **a** SSMF, and when using dispersion management approaches of **b** + NZ-DSF or -NZ-DSF, **c** SSMF and DCF, or **d** SSMF and FBG



direction (a). When employing the dispersion management approaches, the modulated signal is transmitted through + NZ-DSF or - NZ-DSF, which represents direction (b), SSMF and DCF, which represents direction (c), or SSMF and FBG, which represents direction (d). The received laser signal is detected and converted into an electrical signal by a PIN photodetector. The received power spectrum is displayed by using RF spectrum analyzer according to Eq. (5).

The all component parameters with the corresponding numerical values related to LD (quantum well InGaAsP-DFB), SSMF, NZ-DSF, DCF, FBG, and PIN photodetector of the proposed RoF system are listed in Table 1 [2, 3, 56, 57].

### 3 Results and discussion

#### 3.1 Effect of SSMF properties on signal distortions

The influence of the limiting properties of optical fiber, namely attenuation and chromatic dispersion, as well as laser modulation depth  $m$  on the spectrum characteristics of the two-tone modulated laser signal is investigated in Fig. 2a–f. Figure 2a shows the power spectrum of the free-running laser case (i.e., before radiating the fiber) when  $m = 0.3$ . Such a power spectrum is performed with the help of Eq. (5) using the modulated laser output power calculated from Eq. (4). The spectrum illustrates two pronounced peaks, which represent the powers of the two fundamental modulated laser signals at frequencies of  $f_{m1}$  ( $\approx f_r = 25$  GHz) and  $f_{m2}$  ( $f_{m1} + \Delta f$ ,  $\Delta f = 10$  MHz). In addition, the nonlinear 3rd and 2nd intermodulation products ( $f_{m1} - \Delta f$ ,  $f_{m2} + \Delta f$  and  $f_{m1} + f_{m2}$ , respectively) and the 2nd harmonics ( $2f_{m1}$  and  $2f_{m2}$ ) are appeared also in the spectrum of Fig. 2a. The power differences between the laser fundamental signals and the nonlinear distortion products of 3rd, 2nd intermodulation and 2nd harmonics represent the distortions of IMD3, IMD2, and HD2, respectively. These power differences are calculated using Eqs. (8), (7), and (6), respectively. Figure 2b shows the power spectrum of the received fundamental laser signals and distortion products after traveling down a SSMF with length  $L = 2$  km. The dispersion parameter is ignored ( $D = 0$ ), while the attenuation is enabled ( $\alpha_f = 0.2$  dB/km) in order to gain insight into the intrinsic fiber attenuation effect on distortions. This means that the third term in fiber propagation Eq. (10) that represents GVD is ignored, and the calculations are then limited to the first two terms only. The spectrum indicates that there is no significant influence of attenuation on the distortions (i.e., it remains almost constant when compared to the case of free-running laser shown in Fig. 2a). The effect of fiber dispersion along with attenuation at the same modulation conditions of Fig. 2b is illustrated in Fig. 2c. This is achieved when fiber dispersion parameter given in Eq. (11) is enabled with a value of  $D = 16.75$  ps/nm/km (i.e., the calculations include the GVD term in Eq. (10)). The

power spectrum of Fig. 2c reveals that there is a significant decrease in the power differences between the fundamental laser signals and their nonlinear distortion products when compared to the spectrum of Fig. 2b. This indicates a significant increase in the distortion types IMD3, IMD2, and HD2 as a result of enabling fiber dispersion parameter, which reveals the degrading effect of fiber dispersion on distortions. As numeric illustration, IMD3 increases from  $-13.5$  to  $-7.5$  dBc, IMD2 increases from  $-10.2$  to  $-2.9$  dBc, and HD2 increases from  $-16.2$  to  $-8.2$  dBc. Increasing the fiber length to  $L = 5$  km works to increase the distortions to higher levels as illustrated in the spectrum of Fig. 2d. This is due to the fact that increasing the fiber length increases the accumulated fiber dispersion along the fiber, which in turn causes more distortions. At this fiber length, the powers of the fundamental signals and the 3rd intermodulation products are nearly equal (i.e.,  $\text{IMD3} \approx 0$ ). In addition,  $\text{IMD2} = 2.9$  dBc and  $\text{HD2} = -5.2$  dBc. These distortions deteriorate the transmission system performance [14, 15].

Influence of the modulation depth  $m$  at fiber length of 2 and 5 km on the distortion types is illustrated in Fig. 2e and f, respectively. The modulation depth  $m$  is changed in Eq. (3) of injection current  $I(t)$  by varying the modulation current  $I_m$ . Figure 2e confirms that at  $L = 2$  km, when modulation is as deep as  $m = 0.6$ , all distortions increase compared to those in Fig. 2c when  $m = 0.3$  (intermediate). This is due to the fact that when  $m$  increases from 0.3 to 0.6, the signal asymmetry adds to the nonlinear distortion products which then carry more power and approach the fundamental components. This results in an increase in the distortion levels [58], which significantly manifests in IMD3 that degrades the system performance [14, 15]. On the other hand, decreasing  $m$  to 0.1 at  $L = 5$  km works to decrease all distortions to lower levels (see Fig. 2f) when compared to those in Fig. 2e when  $m = 0.3$ , which in turn improves the modulation performance.

Figure 3a and b plots variations of the distortion types when  $m = 0.3$  as functions of the fiber length  $L$ ;  $L$  ranges from  $L = 0$  (i.e., free-running laser case) to 6 km, when the dispersion parameter  $D$  is disabled and enabled, respectively. Figure 3a shows that when  $D$  is disabled, there is no significant variation in all distortion values over the entire used fiber lengths, which confirms that the fiber attenuation does not affect the distortions [24]. This is despite the fact that the increase in fiber length increases the attenuation effect according to Eq. (9). It is also clear from Fig. 3a that the IMD2 is the highest distortion level, while HD2 is the lowest one. When the dispersion parameter is enabled, the dispersion effect on distortions appears significantly as illustrated in Fig. 3b. The figure reveals that the distortions exacerbate as the fiber length increase, which agree with the results reported in [30]. This is mainly due to the dispersion effect that increases with the fiber length.

The influence of the modulation depth  $m$  on the distortions should also be taken into account because of its considerable relationship to the modulated laser output

power  $P(t)$ . This can be explained as follows: The variations in the modulation depth  $m$  cause variations in the injection current  $I(t)$  according to Eq. (3). These injection current variations induce corresponding variations in the carrier density  $N(t)$  and photon density  $S(t)$  inside the laser active region as given in the coupled rate Eqs. (1) and (2). According to Eq. (4), there is a relationship between  $S(t)$  and the modulated laser output power  $P(t)$  of both the fundamental signals and the associated distortion products. Figure 4a, b, and c illustrates the variations of distortion types IMD3, IMD2,

and HD2, respectively, as a function of  $m$ . The distortions are calculated without fiber and when transmitted over SSMF with dispersion and attenuation effects at lengths of  $L = 2$  and 5 km. The figures illustrate that all distortion types increase with the increase in  $m$ , especially for the free-running laser case (without fiber) and at a long fiber of  $L = 5$  km. The increase in distortions with  $m$  in the free-running laser and when transmitted over the fiber agrees with the results reported in [58] and [24], respectively.

**Table 1** Basic components and their parameter values of the proposed simulation model

Component	Parameter	Value
LD	Wavelength, $\lambda$	1.55 $\mu\text{m}$
	Active layer volume, $V$	$3 \times 10^{-11}$ cm <sup>3</sup>
	Group velocity, $v_g$	$8.33 \times 10^9$ cm/s
	Quantum efficiency, $\eta_o$	0.255
	Differential gain coefficient, $a_o$	$9.9 \times 10^{-16}$ cm <sup>2</sup>
	Carrier density at transparency, $N_o$	$1.23 \times 10^{18}$ cm <sup>-3</sup>
	Linewidth enhancement factor, $\alpha$	3.5
	Mode confinement factor, $\Gamma$	0.2
	Photon lifetime, $\tau_p$	$1.69 \times 10^{-12}$ s
	Electron lifetime, $\tau_c$	$776 \times 10^{-12}$ s
	Spontaneous emission factor, $\beta_{sp}$	$3 \times 10^{-5}$
	Gain compression coefficient, $\varepsilon$	$2.77 \times 10^{-17}$ cm <sup>3</sup>
	Threshold current, $I_{th}$	9.8 mA
SSMF	Attenuation coefficient, $\alpha_f$	0.2 dB/km
	Dispersion, $D_{SMF}$	+ 16.75 ps/nm/km
	Dispersion slope, $S_{SMF}$	0.075 ps/nm <sup>2</sup> /km
NZ-DSF	Length, $L_{SMF}$	(1–6) km
	Attenuation coefficient, $\alpha_{NZ-DSF}$	0.185 dB/km
	Dispersion, $D_{NZ-DSF}$	+ 4.5 and – 7.5 ps/nm/km
DCF	Dispersion slope, $S_{NZ-DSF}$	0.01 ps/nm <sup>2</sup> /km
	Length, $L_{NZ-DSF}$	(1–6) km
	Attenuation coefficient, $\alpha_{DCF}$	0.6 dB/km
FBG	Dispersion, $D_{DCF}$	– 82 ps/nm/km
	Dispersion slope, $S_{DCF}$	0.35 ps/nm <sup>2</sup> /km
	Length, $L_{DCF}$	(0.2–1.22) km
PIN	Center wavelength, $\lambda_o$	1.55 $\mu\text{m}$
	Core refractive index, $\tilde{n}$	1.45
	Grating length, $L_g$	20 nm
PIN	Chirp function	Linear
	Responsivity, $R$	1 A/W
PIN	Dark current, $I_d$	10 nA

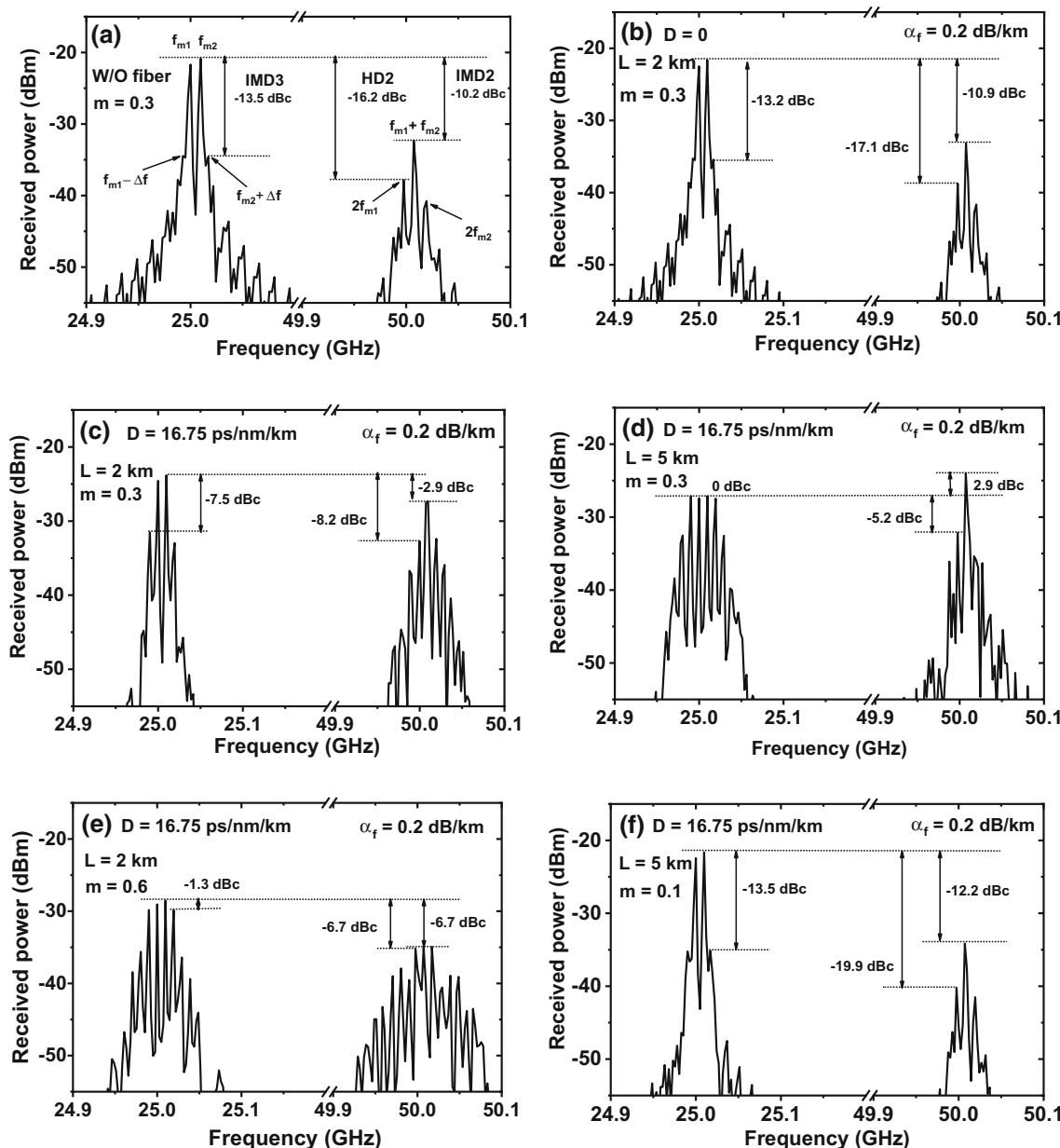
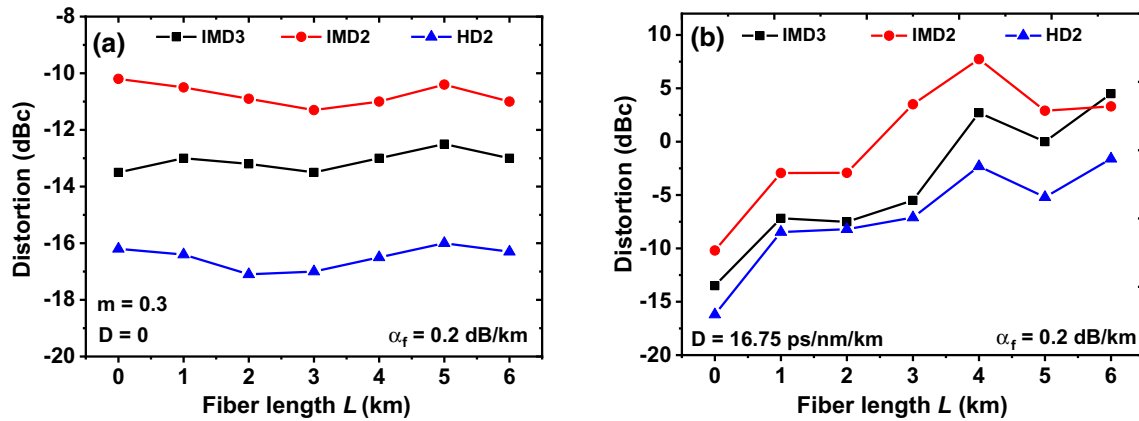


Fig. 2 Frequency domain characteristics of the modulated laser signal under two-tone modulation at different conditions

### 3.2 Effect of dispersion management approaches on signal distortions

From the previous results, it is clear that the main reason for the increase in distortions inside the fiber is dispersion and accordingly, it requires an appropriate approach to reduce it. Figure 5a–j compares the spectra of the received power from SSMF and when using different dispersion management approaches (+ NZ-DSF, – NZ-DSF, FBG, and DCF) at  $m = 0.3$ . Figure 5a and b displays the spectra of the received power from SSMF at lengths of  $L = 2$  and 6 km, respectively. These power spectra confirm that the distortions over SSMF increase as the length increase. When  $L = 6$ , the powers

of the distortion product of the 2nd and 3rd intermodulation increase beyond the fundamental components, which indicates a highest distortion levels, as shown in Fig. 5b. Figure 5c and d displays the received power spectra when SSMF is replaced by + NZ-DSF under the same conditions of Fig. 5a and b, respectively. The spectra illustrate that the use of + NZ-DSF reduces IMD3 when  $L = 2$  km (see Fig. 5c) and has a significant effect when  $L = 6$ ; it reduces all distortion types (see Fig. 5d). On the other hand, the effect of – NZ-DSF is shown in the power spectra of Fig. 5e and f when  $L = 2$  and 6 km, respectively. The spectra indicate that – NZ-DSF acts similar to + NZ-DSF, but with more effective results at  $L = 6$  km as shown in Fig. 5f. Figure 5g



**Fig. 3** Variation of distortion types (IMD3, IMD2, and HD2) when  $m = 0.3$  as a function of fiber length  $L$  when **a** attenuation only is enabled and **b** attenuation and dispersion are enabled

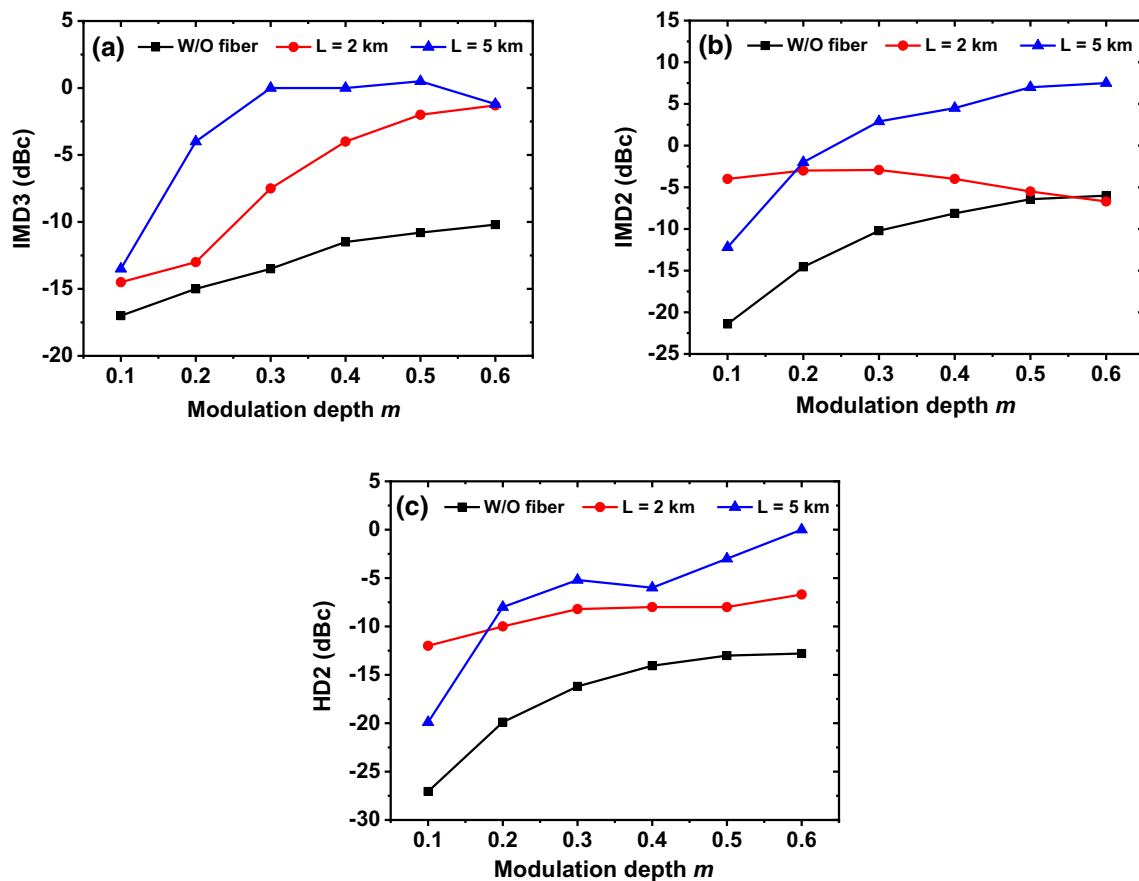


**Fig. 4** Variation of **a** IMD3, **b** IMD2, and **c** HD2 with the laser modulation index  $m$  without fiber and when transmitted over the SSMF with lengths of  $L = 2, 5$  km

and h displays the received power spectra when using FBG after SSMF at  $L = 2$  and  $6$  km, respectively. The FBG is adjusted to reflect the wavelength of  $1.55 \mu\text{m}$  according to Eq. (14). After a round-trip time inside the FBG given by Eq. (15), the anomalous GVD of the SSMF at  $1.55 \mu\text{m}$  can be reduced by the normal GVD of the FBG with a dispersion parameter  $D_g$  given by Eq. (16). The spectra shown in Fig. 5g and h reveal

a significant decrease in all distortions for both fiber lengths when compared to those of SSMF, + NZ-DSF, and - NZ-DSF. The received power spectra when using DCF after SSMF as a dispersion management approach at  $L = 2$  and  $6$  km are illustrated in Fig. 5i and j, respectively. The length  $L_{\text{DCF}}$  of DCF with a normal GVD ( $-82$  ps/nm/km) is adjusted to satisfy the condition in



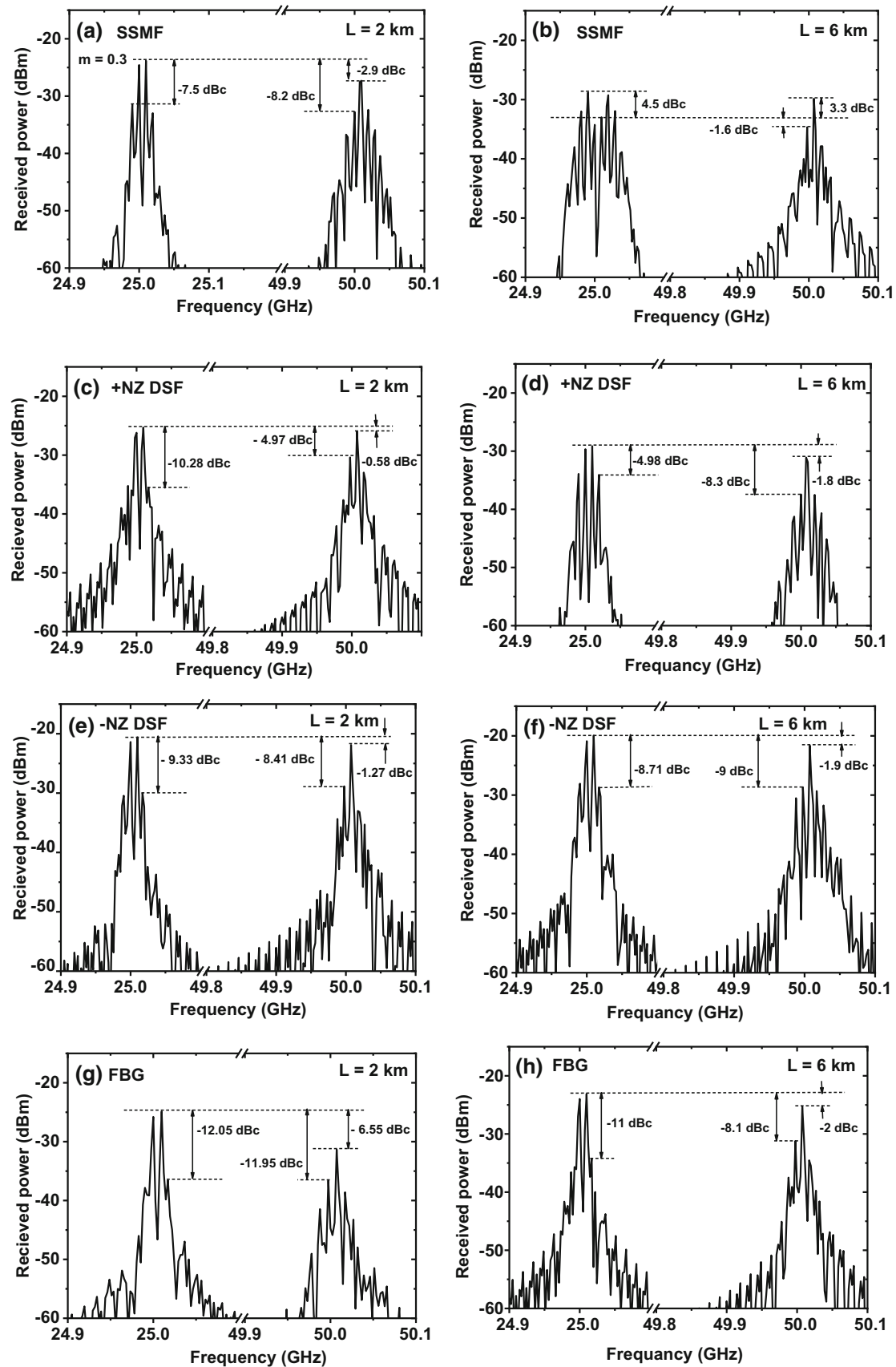


**Fig. 5** Received power spectra of the modulated laser signal under two-tone modulation when  $m = 0.3$  after passing through SSMF (a, b) and after using different dispersion management approaches such as + NZ-DSF (c, d), - NZ-DSF (e, f), FBG (g, h), and DCF (i, j) when  $L = 2$  km (a), (c), (e), (g), (i), and 6 km (b), (d), (f), (h), (j)

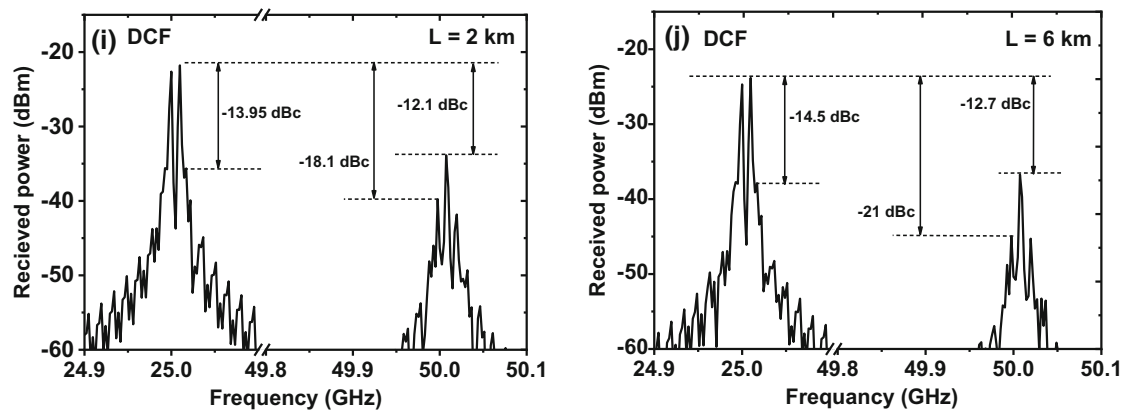


Fig. 5 continued

Eq. (13). This can compensate the anomalous dispersion accumulated along the length of the SSMF. The spectra shown in Fig. 5i and i illustrate a significant reduction in distortions when using DCF compared to using FBG over both fiber lengths. This indicates that the use of DCF after SSMF is more effective than the use of FBG in reducing distortion, which agrees with the findings reported in [59]. For example, when  $L = 2$  km, IMD3, IMD2, and HD2 are reduced from  $-7.5$ ,  $-2.9$ , and  $-8.2$  dBc when using FBG (see Fig. 5a) to  $-13.9$ ,  $-12.1$ , and  $-18.1$  dBc when using DCF (see Fig. 5i), whereas when  $L = 6$  km, these nonlinear distortions are reduced from  $4.5$ ,  $3.3$ , and  $-1.6$  dBc when using FBG (see Fig. 5b) to  $-14.5$ ,  $-12.7$ , and  $-21$  dBc when using DCF (see Fig. 5j), respectively.

The effects of SSMF and the investigated dispersion management approaches on the reduction of distortions IMD3, IMD2, and HD2 are illustrated in Fig. 6a, b, and c, respectively, when  $m = 0.3$  at different fiber lengths ranging from 1 to 6 km. When fiber is as short as  $L = 1$  km, the effects of all dispersion management approaches on IMD3 reduction are almost similar and more effective as illustrated in Fig. 6a. As the fiber length increases, the effects change so that the use of DCF becomes the more effective approach than the others. Figure 6b reveals that the effects of both FBG and DCF on IMD2 reduction are more effective up to  $L < 3$  km, while both  $-NZ$ -DSF and DCF are more effective when  $L \geq 3$  km, taking into consideration that the use of DCF is the most effective approach over the entire fiber lengths. The reduction of distortions has been also predicted with the use of  $-NZ$ -DSF in [30] for cable television transport systems. The dispersion management approaches for reducing IMD2 exhibit almost similar behavior for HD2 reduction as illustrated in Fig. 6c. In general, when  $m = 0.3$ , using DCF with SSMF is the most effective approach for reducing all types of distortion, while the use of  $+NZ$ -DSF instead of SSMF is the least effective when compared to the other used approaches over the entire range of the fiber length.

Figure 7a–f shows the influences of SSMF and dispersion management approaches on distortions when  $L = 2$  and 6 km as functions of the modulation depth

$m$  ranges between 0.1 and 0.6. According to Eq. (3), the variations in  $m$  cause variations in the injection current  $I(t)$ . These  $I(t)$  variations cause corresponding variations in the carrier density  $N(t)$  and photon density  $S(t)$  as given in the coupled rate Eqs. (1) and (2). These  $S(t)$  variations cause corresponding variations in the laser output power  $P(t)$  of both the fundamental signals and the associated distortion products according to Eq. (4). Figure 7a and b reveals that IMD3 increases with the increase of  $m$  when  $L = 2$  and 6 km, respectively. This increase in IMD3 is reduced when the dispersion is more managed. For example, when  $L = 2$  km, the increase of  $m$  from 0.1 to 0.6 results in increasing IMD3 from  $-14.5$  to  $-1.3$  dBc without dispersion management (i.e., at SSMF), while it increases from  $-16$  to  $-14.3$  dBc when using DCF, which is the most effective management approach (see Fig. 7a). Also, when  $L = 6$  km, IMD3 increases from  $-14$  to  $-2.3$  dBc at SSMF and increases from  $-17$  to  $-15.5$  dBc when using DCF (see Fig. 7b). The figures reveal also that the effect of all dispersion management approaches is almost similar and less effective when  $m = 0.1$  (small-signal laser modulation case). Moreover, the use of DCF approach is the most effective approach for IMD3 reduction regardless of the value of  $m$ . On the other hand, the SSMF and the dispersion management approaches exhibit almost similar behavior to IMD2 and HD2 over the entire  $m$  range as illustrated in Fig. 7c and e at  $L = 2$  km, and in Fig. 7d and f when  $L = 6$  km, respectively. Up to  $m = 0.3$ , the use of DCF is the best approach for IMD2 and HD2 reduction, and the next is the use of FBG, which gives better performance when  $m \geq 0.4$  at  $L = 2$  km as illustrated in Fig. 7c and e, respectively. The reduction of HD2 with the use of FBG has been reported also in [35] for cable television systems. When  $L = 6$  km, using DCF gives better performance for IMD2 and HD2 reduction up to  $m = 0.5$  compared to the other approaches, as illustrated in Fig. 7d and f, respectively.

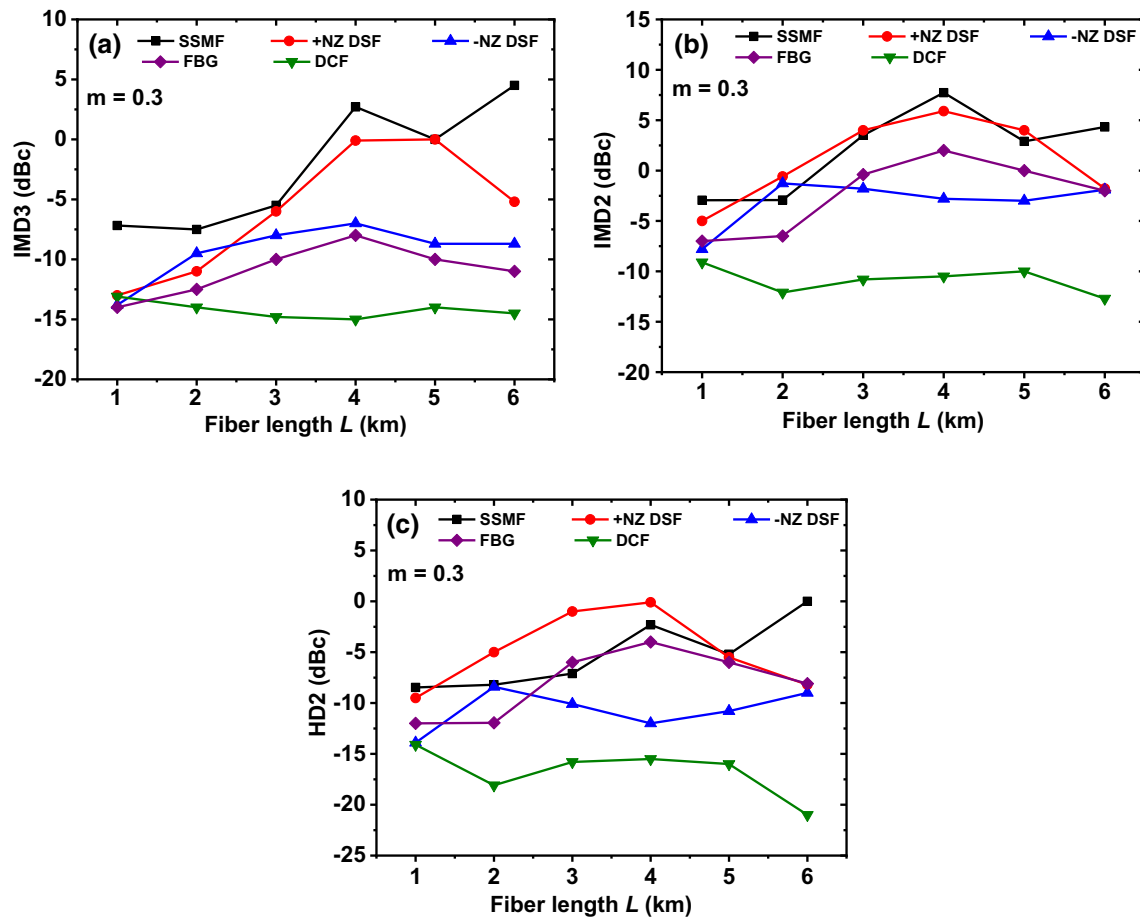


**Fig. 6** Variation of **a** IMD3, **b** IMD2 and **c** HD2 as a function of  $L$  when  $m = 0.3$  at SSMF (black line with squares), +NZ-DSF (red line with circles), -NZ-DSF, FBG, and DCF

### 4 Conclusions

We successfully investigated via numerical modeling and simulation the influences of SSMF properties, and the different dispersion management approaches on the distortion types IMD3, IMD2, and HD2 associated with two-tone modulation of laser diode for use in RoF links. The SSMF properties include attenuation and dispersion, while the dispersion management approaches include +NZ-DSF, -NZ-DSF, FBG, and DCF. The laser was directly modulated with two frequencies of 25 and 25.1 GHz at different modulation depths ranging from  $m = 0.1$  to 0.6. The modulated laser signals with their distortion products were then propagated through fiber at different lengths ranging from  $L = 1$  to 6 km. The received power spectra from the SSMF and the dispersion management approaches were intensively investigated.

The obtained results revealed the following. Regarding effects of SSMF properties, all distortion types are exacerbated as the fiber length increases, which is mainly due to the degrading effect of chromatic dispersion. Also, the distortion types increase as the modulation depth  $m$  increases, especially at longer

fibers. Regarding the effects of dispersion management approaches, they give almost similar effects on IMD3 reduction when  $L = 1$  km, whereas the use of DCF is more effective than the others when  $L = 6$  km. The dispersion management approaches used for reducing the IMD2 exhibit almost similar behavior for HD2 reduction. The use of FBG and DCF is more effective for IMD2 and HD2 reduction up to  $L < 3$  km, while the use of -NZ-DSF and DCF is more effective when  $L \geq 3$  km. In general, up to  $m = 0.3$ , the use of DCF is the most effective approach for reducing all signal distortion types over the entire used fiber length range (1–6 km), while the use of +NZ-DSF is the least effective. When  $L = 2$  km, the use of FBG is the most effective approach for IMD2 and HD2 reduction when  $m \geq 0.4$ , whereas when  $L$  is increased to 6 km, the use of DCF is the most effective approach up to  $m = 0.5$ . Finally, the effect of dispersion management approaches for distortion reduction is minimal when  $m$  is small as 0.1.

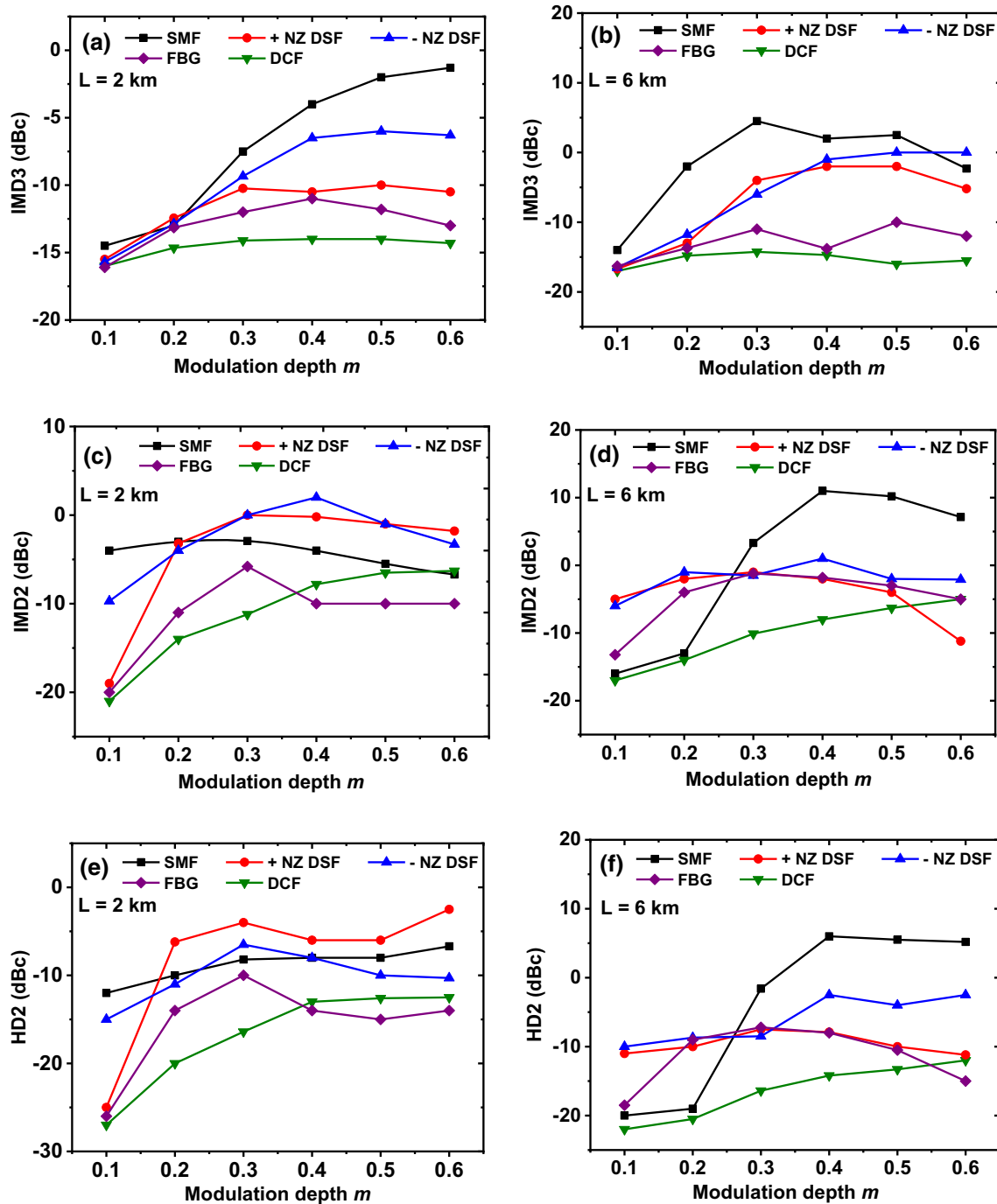


**Fig. 7** Variation of IMD3 (a, b), IMD2 (c, d) and HD2 (e, f) as a function of  $m$  at  $L = 2$  km (a), (c), (e), and (g), and at  $L = 6$  km (b), (d), (f), and (h), for SSMF, + NZ-DSF, - NZ-DSF, FBG, and DCF

**Acknowledgements** Not applicable.

**Authors' contribution**

AM contributed to conceptualization, formal analysis, investigations, writing—review and editing, and visualization. YAE-S was involved in formal analysis, investigations, and

writing—original draft. MA and TM contributed to writing—review, and supervision.

**Funding** Open access funding provided by The Science, Technology & Innovation Funding Authority (STDF) in cooperation with The Egyptian Knowledge Bank (EKB). Not applicable.

**Data Availability Statement** This manuscript has no associated data, or the data will not be deposited. [Authors' comment: The data sharing is not applicable to this article as no datasets were generated or analyzed during the current study.]

## Declarations

**Conflict of interest** The authors declare that they have no known competing financial interests or personal relationships that could have appeared to influence the work reported in this paper.

**Ethical approval** Not applicable.

**Consent to participate** Not applicable.

**Consent for publication** Not applicable.

**Open Access** This article is licensed under a Creative Commons Attribution 4.0 International License, which permits use, sharing, adaptation, distribution and reproduction in any medium or format, as long as you give appropriate credit to the original author(s) and the source, provide a link to the Creative Commons licence, and indicate if changes were made. The images or other third party material in this article are included in the article's Creative Commons licence, unless indicated otherwise in a credit line to the material. If material is not included in the article's Creative Commons licence and your intended use is not permitted by statutory regulation or exceeds the permitted use, you will need to obtain permission directly from the copyright holder. To view a copy of this licence, visit <http://creativecommons.org/licenses/by/4.0/>.

## References

1. X.N. Fernando, *Radio Over Fiber for Wireless Communications: From Fundamentals to Advanced Topics* (John Wiley & Sons, 2014)
2. G.P. Agrawal, *Fiber-Optic Communication System* (A John Wiley & Sons. Inc., Publication, New York, 2002)
3. K. Sato, S. Kuwahara, Y. Miyamoto, Chirp characteristics of 40-Gb/s directly modulated distributed-feedback laser diodes. *J. Lightwave Technol.* **23**(11), 3790 (2005)
4. P.J. Urban, G.C. Amaral, J.P. von der Weid, Fiber monitoring using a sub-carrier band in a sub-carrier multiplexed radio-over-fiber transmission system for applications in analog mobile fronthaul. *J. Lightwave Technol.* **34**(13), 3118–3125 (2016)
5. C.H. Lee, *Microwave Photonics ed* (Taylor & Francis, New York, NY, 2013)
6. A. Bakry, M. Ahmed, Harmonic and intermodulation distortions and noise associated with two-tone modulation of high-speed semiconductor lasers. *Phys. Wave Phenom.* **24**(1), 64–72 (2016)
7. A. Bakry, Modeling of millimeter-wave modulation characteristics of semiconductor lasers under strong optical feedback. *Sci. World J.* **2014**, 1–9 (2014)
8. D. Wake, A. Nkansah, N.J. Gomes, G. de Valicourt, R. Brenot, M. Violas, S. Pato, A comparison of radio over fiber link types for the support of wideband radio channels. *J. Lightwave Technol.* **28**(16), 2416–2422 (2010)
9. G. Qazi, A.K. Sharma, M. Uddin, Investigation on intermodulation products (IMPs) for IM-DD SCM optical links. *Optik* **125**(5), 1629–1633 (2014)
10. K. Zhang, Q. Zhuge, H. Xin, W. Hu, D.V. Plant, Performance comparison of DML, EML and MZM in dispersion-unmanaged short reach transmissions with digital signal processing. *Opt. Express* **26**(26), 34288–34304 (2018)
11. S. Odermatt, B. Witzigmann, B. Schmithüsen, Harmonic balance analysis for semiconductor lasers under large-signal modulation. *Opt. Quantum Electron.* **38**(12), 1039–1044 (2006)
12. G. Morthier G, P. Vankwikelberge, *Handbook of Distributed Feedback Laser Diodes*. (Artech House, 2013)
13. C.Y. Kuo, M.S. Lin, S.J. Wang, D.A. Ackerman, L.J.P. Ketelsen, Static and dynamic characteristics of DFB lasers with longitudinal nonuniformity. *IEEE Photonics Technol. Lett.* **2**(7), 461–463 (1990)
14. K.Y. Lau, A. Yariv, Intermodulation distortion in a directly modulated semiconductor injection laser. *Appl. Phys. Lett.* **45**(10), 1034–1036 (1984)
15. H.H. Lu, Y.P. Lin, M.C. Lin, Nonlinear distortion analysis for directly modulated dfb laser diode in CATV systems. *J. Opt. Commun* **22**, 1–3 (2001)
16. P.A. Morton, R.F. Ormondroyd, J.E. Bowers, M.S. Demokan, Large-signal harmonic and intermodulation distortions in wide-bandwidth GaInAsP semiconductor lasers. *IEEE J. Quantum Electron.* **25**(6), 1559–1567 (1989)
17. S.W. Mahmoud, A. Mahmoud, Relative intensity noise and nonlinear distortions of semiconductor laser under analog modulation for use in CATV systems. *Int. J. New Horiz. Phys.* **2**(2), 37–45 (2015)
18. J.S. Gustavsson, A. Haglund, C. Carlsson, J. Bengtsson, A. Larsson, Harmonic and intermodulation distortion in oxide-confined vertical-cavity surface-emitting lasers. *IEEE J. Quantum Electron.* **39**(8), 941–951 (2003)
19. G. Tartarini, A. Lena, D. Passaro, L. Rosa, S. Selleri, P. Faccin, E.M. Fabbri, Harmonic and intermodulation distortion modeling in IM-DD multi-band radio over fiber links exploiting injection locked lasers. *Opt. Quantum Electron.* **38**(9), 869–876 (2006)
20. M. Ahmed, A. El-Lafi, Large-signal analysis of analog intensity modulation of semiconductor lasers. *Opt. Laser Technol.* **40**(6), 809–819 (2008)
21. A. Bakry, M. Ahmed, Influence of sinusoidal modulation on mode competition and signal distortion in multimode InGaAsP lasers. *Opt. Laser Technol.* **50**, 134–140 (2013)
22. P. Westbergh, E. Söderberg, J.S. Gustavsson, A. Larsson, Z. Zhang, J. Berggren, M. Hammar, Noise, distortion and dynamic range of single mode 1.3  $\mu\text{m}$  InGaAs vertical cavity surface emitting lasers for radio-over-fibre links. *IET Optoelectron.* **2**(2), 88–95 (2008)
23. A. Ng'oma, Radio-over-fibre technology for broadband wireless communication systems (Technische Universiteit Eindhoven, 2005)
24. M. Ahmed, Y. Al-Hadeethi, G. Alghamdi, Influence of fiber properties on harmonic and intermodulation distortions of semiconductor lasers. *J. Eng. Res. Rep.* **20**(7), 56–67 (2021)

25. G. Meslener, Chromatic dispersion induced distortion of modulated monochromatic light employing direct detection. *IEEE J. Quantum Electron.* **20**(10), 1208–1216 (1984)
26. C.S. Oh, W. Gu, Fiber induced distortion in a subcarrier multiplexed lightwave system. *IEEE J. Sel. Areas Commun.* **8**(7), 1296–1303 (1990)
27. M.R. Phillips, T.E. Darcie, D. Marcuse, G.E. Bodeep, N.J. Frigo, Nonlinear distortion generated by dispersive transmission of chirped intensity-modulated signals. *IEEE Photonics Technol. Lett.* **3**(5), 481–483 (1991)
28. E.E. Bergmann, C.Y. Kuo, S.Y. Huang, Dispersion-induced composite second-order distortion at 1.5  $\mu\text{m}$ . *IEEE Photonics Technol. Lett.* **3**(1), 59–61 (1991)
29. P. Krehlik, Characterization of semiconductor laser frequency chirp based on signal distortion in dispersive optical fiber. *Opto-Electron. Rev.* **14**(2), 119–124 (2006)
30. H.H. Lu, J.W. Liaw, Y.S. Lee, W.L. Tsai, Y.J. Ji, Directly modulated cable television transport systems using negative dispersion fiber. *Opt. Eng.* **44**(3), 030501 (2005)
31. M. Jaworski, M. Marciniak, M. Long distance analog CATV link utilizing non-zero dispersion-shifted fiber. In: 2000 2nd international conference on transparent optical networks. Conference proceedings (Cat. No. 00EX408) (IEEE, 2000, June), pp. 107–110
32. D. Piehler, C. Y. Kuo, J. Kleefeld, C. Gall, Nonlinear intermodulation distortion in an optically amplified analog video transport system with dispersion compensating fiber. In: Proceedings of European conference on optical communication, vol. 3, (IEEE, 1996 September), pp. 217–220
33. H. Yoshinaga, E. Yoneda, 40-Channel VSB-AM video transmission through 70 km of high-dispersion fiber by using dispersion-compensating fiber. In: Optical fiber communication conference (Optical Society of America, 1995, February), p. TuN6
34. M. Onishi, H. Ishikawa, M. Shigematsu, H. Kanamori, M. Nishimura, Dispersion-compensating fiber with high figure of merit and its application to an analog transmission system. In: Optical fiber communication conference (Optical Society of America, 1994 February), p. ThK1
35. Q. Ye, F. Liu, R. Qu, Z. Fang, Analysis of dispersion compensation by chirped fiber grating in directly and externally modulated CATV systems. *Optik* **118**(12), 579–583 (2007)
36. H. Wang, W. Zhu, Chirped fiber gratings for dispersion compensation in lightwave CATV systems. *Int. J. Infrared Millim. Waves* **22**(11), 1633–1641 (2001)
37. J. Marti, D. Pastor, M. Tórtola, J. Capmany, A. Montero, On the use of tapered linearly chirped gratings as dispersion-induced distortion equalizers in SCM systems. *J. Lightwave Technol.* **15**(2), 179–187 (1997)
38. M.B. Hossain, A. Adhikary, T.Z. Khan, Performance investigation of different dispersion compensation methods in optical fiber communication. *Asian J. Res. Comput. Sci.* **5**(2), 36–44 (2020)
39. M. M. Abbood, H. M. Al-Tamimi, B. J. Hamza, Y. M. Abid, A. H. Ali, M. A. Al-Ja'afari, M. A. Al-rubei, Dispersion compression for different optic communication systems using DCF and FBG. In: AIP conference proceedings, (AIP Publishing LLC, 2021 October), 2404(1):080030
40. S. Kumar, S. Sharma, S. Dahiya, Wdm-based 160 gbps radio over fiber system with the application of dispersion compensation fiber and fiber Bragg grating. *Front. Phys.* **9**, 691387 (2021)
41. S. Aggarwal, N. Garg, G. Kaur, Performance evaluation of various dispersion compensation modules. *Wirel. Pers. Commun.* **123**(3), 2011–2025 (2022)
42. I. Nsengiyumva, E. Mwangi, G. Kamucha, Performance analysis of a linear Gaussian-and tanh-apodized FBG and dispersion compensating fiber design for chromatic dispersion compensation in long-haul optical communication networks. *Int. J. Opt.* **2022**, 1–4 (2022)
43. P. Corvini, T. Koch, Computer simulation of high-bit-rate optical fiber transmission using single-frequency lasers. *J. Lightwave Technol.* **5**(11), 1591–1595 (1987)
44. M. Ahmed, Numerical approach to field fluctuations and spectral lineshape in InGaAsP laser diodes. *Int. J. Numer. Model. Electron. Netw. Dev. Fields* **17**(2), 147–163 (2004)
45. M.J. Potasek, G.P. Agrawal, Self-amplitude-modulation of optical pulses in nonlinear dispersive fibers. *Phys. Rev. A* **36**(8), 3862 (1987)
46. G.P. Agrawal, *Nonlinear Fiber Optics* (Academic Press, San Diego, 2001)
47. O.V. Sinkin, R. Holzlöhner, J. Zweck, C.R. Menyuk, Optimization of the split-step Fourier method in modeling optical-fiber communications systems. *J. Lightwave Technol.* **21**(1), 61 (2003)
48. F. Thabat, Performance of high speed laser diodes in optical fiber communication systems. (M.Sc) Faculty of Science. (King Abdulaziz University, 2013)
49. International Telecommunication Union (ITU), Telecommunication standardization sector, Series G: Transmission systems and media, digital systems and networks, Recommendation ITU-T G.655, “Characteristics of a non-zero dispersion-shifted single-mode optical fiber and cable”, approved on 13 November 2009
50. N. Kumano, K. Mukasa, M. Sakano, H. Moridaira, Development of a non-zero dispersion-shifted fiber with ultra-low dispersion slope. *Furukawa Rev.* **22**(1), 1–6 (2002)
51. P. Krehlik, Directly modulated lasers in negative dispersion fiber links. *Opto-Electron. Rev.* **15**(2), 71–77 (2007)
52. P.B. Harboe, E. da Silva, J.R. Souza, Analysis of FWM penalties in DWDM systems based on G. 652, G. 653, and G. 655 optical fibers. *Int. J. Electr. Comput. Energ. Electron. Commun. Eng.* **2**(12), 2674–2680 (2008)
53. A.J. Antos, D.K. Smith, Design and characterization of dispersion compensating fiber based on the LP/sub 01/mode. *J. Lightwave Technol.* **12**(10), 1739–1745 (1994)
54. J. Liu, Y.L. Lam, Y.C. Chan, Y. Zhou, J. Yao, Fabrication of high-performance dispersion compensating fiber by plasma chemical vapor deposition. *Fiber Integr. Opt.* **18**(2), 63–67 (1999)
55. L. Grüner-Nielsen, S.N. Knudsen, B. Edvold, T. Veng, D. Magnussen, C.C. Larsen, H. Damsgaard, Dispersion compensating fibers. *Opt. Fiber Technol.* **6**(2), 164–180 (2000)

56. M.I. Hayee, A.E. Willner, NRZ versus RZ in 10–40-Gb/s dispersion-managed WDM transmission systems. *IEEE Photonics Technol. Lett.* **11**(8), 991–993 (1999)
57. R. Kashyap, *Fiber bragg gratings* (Academic press, 2009)
58. S.W. Mahmoud, A. Mahmoud, M. Ahmed, Noise performance and nonlinear distortion of semiconductor laser under two-tone modulation for use in analog CATV systems. *Int. J. Numer. Model. Electron. Netw. Dev. Fields* **29**(2), 280–290 (2016)
59. M. Ahmed, M. Yamada, M. Saito, Numerical modeling of intensity and phase noise in semiconductor lasers. *IEEE J. Quantum Electron.* **37**(12), 1600–1610 (2001)